ASM Sc. J., 12, Special Issue 4, 2019 for ICSE2018, 36-45

Modelling approach from Cell to Panel Size for CIGS Solar utilizing Silvaco TCAD and Matlab Software

A.H. Hasani[1*], S.F. Abdullah[2], F. Za'abar[1], M.S. Bahrudin[1], M. Mansor[2] and A.W.M. Zuhdi[1]

[1]*Institute of Sustainable Energy (ISE), Universiti Tenaga Nasional, Kajang, Malaysia*

[2]*Dept. of Electrical and Electronics Engineering, College of Engineering, Universiti Tenaga Nasional, Kajang, Malaysia*

Conventionally, simulation and performance analysis of solar cells are conducted at cell level only. This paper presents a modelling approach that enables continuous performance evaluation of a solar cell from cell level to the system level. In the first stage of this work, a Cu(In, Ga)Se2 (CIGS) solar cell device structure is developed using Technology Computer-Aided Design (TCAD) software. In order to design a high-performance CIGS solar cell, material properties such as layer thickness and doping concentration are optimized with respect to the cells' efficiency within the ranges reported in the literature. Performance analysis of the TCAD model is then conducted and the electrical characteristics of the model are obtained. Matlab is used to post-process the electrical data in order to develop an equivalent one-diode electrical model from the TCAD model. The performance of the one-diode model in representing the TCAD model is validated at different temperatures and from the current-voltage (I-V) characteristic curves of both models, it is observed that the one-diode model is able to represent the TCAD model with great accuracy. The I-V curves coincide at the three main points such as the short-circuit current (Isc), the maximum power point (MPP), and the open-circuit voltage (Voc) with minimal error gaps along the I-V curve. As a conclusion, the one-diode model can be used in system-level simulations to observe the performance of the solar cell.

Keywords: CIGS solar cell; modelling approach; TCAD; system level; Matlab; one-diode

I. INTRODUCTION

Renewable energy is getting more attention nowadays since fossil-based energy is bound to deplete with time. Furthermore, renewable energy such as solar energy is unlimited in resource since it comes from the sun and is available throughout the year. Briefly, solar photovoltaic (PV) is associated with the conversion of energy from solar to electrical with the use of semiconductor materials known as solar cells. Through this concept, power generation systems based on solar PV are introduced which can be implemented to support the main power grid (grid-connected) or as a stand-alone power system (off-grid).

In recent years, researchers have spent a lot of effort in order to maximize the output power generated by the solar PV power generation systems. The effort covers every part of a solar PV power generation system. For example, an off-grid power system based on solar PV is shown in Figure 1. Referring to Figure 1, there are generally three main components that form a solar PV power system apart from the load. They are the PV power source, the unidirectional DC-DC converter, and the bus voltage regulator. Each of these components contribute to the output power generated by the system. Generally, research on the unidirectional DC-DC converter requires input from the PV power source. This is done by utilizing the parameters of the PV power source obtained from the datasheet provided by the manufacturer (Ahmed and Salam, 2018).

*Corresponding author's e-mail: azri.husni@uniten.edu.my

The PV power source is known as a PV array which is formed by wiring PV modules in parallel and series to achieve the desired output power. Similarly, PV modules are a group of solar cells interconnected together. Hence, in order to improve the performance of the PV power source, there are a huge number of research done to improve the efficiency since the maximum output power generated by the solar cell is directly proportional to the efficiency of the cells. The research includes the development of solar cells from various materials and by utilizing different processes (Green *et al.*, 2018). Conventionally, the development of solar cells and their performance evaluation are conducted at the cell level. This approach can be observed from the majority of the research which involves modelling and simulation of solar cells. There is usually no continuity between the development of the solar cell to the implementation of the solar cell at the system level simulations.

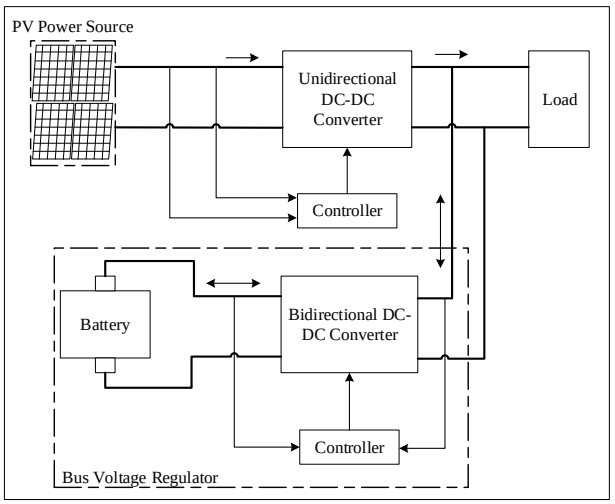

Figure 1. Off-Grid Power Generation System based on Solar PV

Despite the usual practice of modelling and simulation of solar cells at the cell level, researchers have also shown a lot of interest in replicating or reproducing the I-V characteristics of a solar module in the form of an electrical circuit. Some notable research include the implementation of one-diode model, two-diode model, and three-diode model to reproduce the I-V characteristics of the solar module such as shown in Figure 2 where the electrical circuit models (one-diode, two-diode, three-diode) were developed based on the main electrical parameters that are available from the PV module datasheet (Nishioka *et al.*, 2007; Villalva, Gazoli and Ruppert, 2009a; Ishaque, Salam and Taheri, 2011). These electrical characteristics are such as the nominal open-circuit voltage ($V_{oc,n}$), the nominal short-circuit current ($I_{sc,n}$), the voltage at MPP (V_{mp}), the current at MPP (I_{mp}), and the temperature coefficients (K_V and K_I).

With the capability to replicate and reproduce the I-V characteristics of the solar module, it is possible to implement similar methods on solar cells. An equivalent electrical circuit can also be developed based on the electrical parameters of a solar cell. Through this, modelling and simulation of solar cells can be extended up to the system-level simulation and the performance of the solar cells can be evaluated in the form of PV modules and also PV array. In this paper, a modelling approach to observe and evaluate the performance of solar cells at system level simulation is presented. This approach is applicable to different types of solar cells. In this work, we chose thin-film solar cell technology in particular CIGS due to the promise of high performance, combined with low cost that it holds even though silicon-based solar panels account for more than 90% of the production. Current record efficiency of CIGS cell is 22.9% (John Parnell, 2017), leading other thin-film alternatives. This can be attributed to its high absorption coefficient and large band-gap range since the band-gap can be tuned with the variation of Gallium (Ga) composition in the alloy. Initially, CIGS solar cell is designed based on optimized material properties in order to obtain maximum conversion efficiency, followed by a performance evaluation of the solar cell with TCAD software. Silvaco is widely used for semiconductor device simulation as it contains the required module to characterize the electrical performance of a semiconductor device. The resulting electrical characteristics of the solar cell from the TCAD model is fed to Matlab to perform data processing and system-level simulations. An equivalent one-diode model such as shown in Figure 2 is developed based on the electrical data which could be integrated into solar PV system simulations.

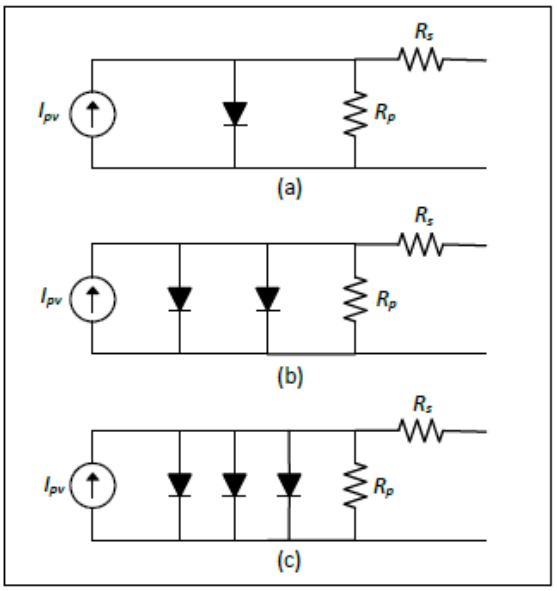

Figure 2. Electrical circuit representation of solar module. (a) One-Diode model, (b) Two-Diode model, (c) Three-Diode model

II. SOLAR CELL DEVICE DEVELOPMENT

Solar cell device development governs the material, process, and structure optimization of the solar cell. For a thin-film CIGS solar cell, this includes identifying the baseline parameters of the layers that will produce an optimized I-V characteristic. The following subsection describes in detail on the parameters that affect the electrical performance of a thin-film CIGS solar cell.

A. Selection of Optimized Baseline Parameters for CIGS Solar Cell

A typical CIGS solar cell structure as depicted in Figure 3 consists of a top contact, followed by a window layer (doped zinc oxide, n-ZnO), an n-type buffer layer (cadmium sulfide, CdS), a p-type absorber layer (CIGS), and Molybdenum (Mo) as the back contact. Soda-lime glass is commonly used as the substrate for the cell. Numerous properties of the materials used in this structure could be tailored for an efficient solar cell. Hence, in this modelling approach, the influence of thickness and carrier concentration of the absorber-buffer-window region on the photovoltaic performance of CIGS solar cell will be first reviewed to determine optimized values for each parameter (Za'abar *et al.*, 2018).

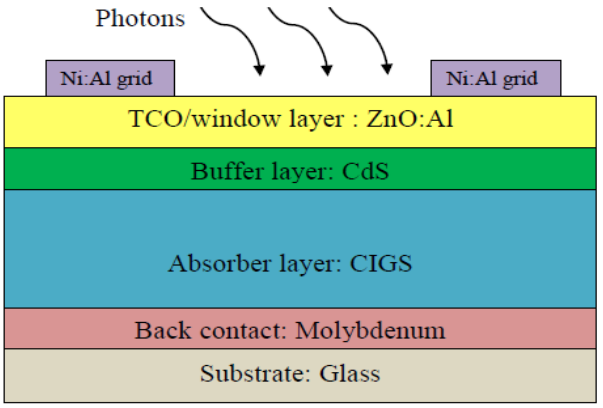

Figure 3. Typical structure of a thin-film CIGS solar cell (Za'abar *et al.*, 2018)

Similarly, a thin and transparent CdS buffer layer will help in allowing more sunlight to be absorbed into the absorber layer. It was found that increased buffer layer thickness causes the electrical parameters of the cell to decrease except for the open-circuit voltage which remains constant (Benmir and Aida, 2013; Heriche, Rouabah and Bouarissa, 2016; Za'abar *et al.*, 2018). This is because short-wavelength photons are absorbed in this layer before reaching the absorber layer. These absorbed photons will not contribute significantly to the generation of electron-hole pairs and eventually to the collected photo-current. However, due to the limitation in fabrication techniques, the thickness limit of CdS buffer layer is no less than 40 nm. Consequently, the suggested optimum thickness of the CdS buffer layer is between 40 nm to 60 nm (Benmir and Aida, 2013; Heriche, Rouabah and Bouarissa, 2016; Za'abar *et al.*, 2018).

Unlike the first two layers, the absorber layer needs to be relatively as the performance of a CIGS solar cell increases with the thickness of the absorber layer. With a thicker absorber layer, more photons with longer wavelengths can be collected which will contribute to higher electrical performance, particularly the current density of the cell. However, there is a limit to the thickness of the absorber layer as too thick of the layer will be a waste of material and will eventually promote recombination. It was also found that thickness of more than 3000 nm does not produce a major increase in the cell efficiency. Hence, the optimum thickness of CIGS absorber layer is determined to be in between 2000 nm to 3000 nm range (Khoshsirat *et al.*,

2015; Za'abar *et al.*, 2018).

In terms of doping concentration, for ZnO the cell efficiency increases with respect to the increment of the concentration of the donor, N_D until it becomes almost constant at doping concentration of $1x10^{18}$ cm^{-3} (Shamim *et al.*, 2015; Heriche, Rouabah and Bouarissa, 2016; Dabbabi, Nasr and Kamoun-Turki, 2017; Za'abar *et al.*, 2018). The increment in cell-efficiency is caused by the improved collection of photo-generated carriers at higher doping concentration. Similar trend can be observed for the CdS doping concentration, but at above $1x10^{17}$ cm^{-3}, the cell efficiency only increases slightly then it starts to decrease when N_D becomes higher (Abdul *et al.*, 2012; Dabbabi, Nasr and Kamoun-Turki, 2017; Sylla, Touré and Vilcot, 2017; Za'abar *et al.*, 2018). Finally, the concentration of the acceptor, N_A for the CIGS absorber layer is found to peak out at $1x10^{16}$ cm^{-3}, before the cell efficiency starts to decrease. This is caused by the recombination process occurring in the back contact (Fathil *et al.*, no date; Abdul *et al.*, 2012; Shamim *et al.*, 2015; Heriche, Rouabah and Bouarissa, 2016; Za'abar *et al.*, 2018).

III. CIGS SOLAR CELL SIMULATION USING SILVACO TCAD SOFTWARE

CIGS solar cell was designed with a structure as shown in Figure 4 using ATLAS interface in Silvaco. Silvaco was used as a simulation tool due to its ability to generate files from mesh, material and doping information for modeling the photovoltaic cell. Following conventional CIGS structure, three main layers in this design are n-type ZnO window layer, n-type CdS buffer layer, and p-type CIGS absorber layer, sandwiched between Aluminum (Al) front contact and Molybdenum (Mo) back contact.

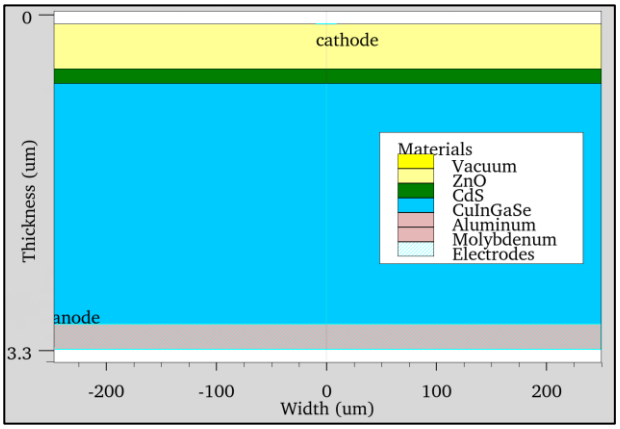

Figure 4. Schematic CIGS solar cell structure designed for simulation using Silvaco (Za'abar *et al.*, 2018)

Based on earlier literature as discussed in Section 2, parametric sweep over the thickness and doping concentration of the three main layers (ZnO, CdS, and CIGS) was first performed to propose an optimized baseline parameter. These parameters, as shown in Table 1 were used in the solar cell design. Other input parameters that are not discussed here were directly selected from literature (Khoshsirat *et al.*, 2015; Mostefaoui *et al.*, 2015; Heriche, Rouabah and Bouarissa, 2016; Za'abar *et al.*, 2018).

The non-linear I-V curve of the TCAD model simulated under standard test condition (STC) is shown in Figure 5. The STC is also known as the nominal condition, which indicates the solar cell temperature of 25 °C and irradiance of 1000 W/m² with air mass 1.5 (AM 1.5) spectrum. It is observed that the I_{sc}, V_{oc}, I_{mp}, and V_{mp} of the cell are 0.0353 A, 0.747 V, 0.0336 A, and 0.619 V respectively. These four electrical parameters are then used to develop an electrical circuit representation of the TCAD model using Matlab. Besides that, an output log file is also available from Silvaco TCAD which contains all the electrical parameters of the TCAD model.

Table 1. Optimized baseline parameters for CIGS solar cell (Za'abar *et al.*, 2018)

Parameters		**Layers**		
		ZnO	***CdS***	***CIGS***
Thickness	Sweep range (nm)	100-200	25-75	2000-4000
	Optimized value (nm)	150	50	2500
Donor concentration, N_D	Sweep range (cm^{-3})	$1x10^{16}$ - $1x10^{18}$	$1x10^{16}$ - $1x10^{18}$	0
	Optimized value (cm^{-3})	$1x10^{18}$	$1x10^{17}$	0

Parameters		Layers		
		ZnO	*CdS*	*CIGS*
Acceptor concentration, N_A	Sweep range (cm^{-3})	0	0	$1x10^{16}$ - $1x10^{18}$
	Optimized value (cm^{-3})	0	0	$1x10^{16}$
Bandgap, E_g (eV)		3.3	2.4	1.27
Conduction band effective density of states, N_C (cm^{-3})		2.2 $x10^{18}$	2.2 $x10^{18}$	2.2 $x10^{18}$
Valence band effective density of states, N_V (cm^{-3})		1.8 $x10^{19}$	1.8 $x10^{19}$	1.8 $x10^{19}$

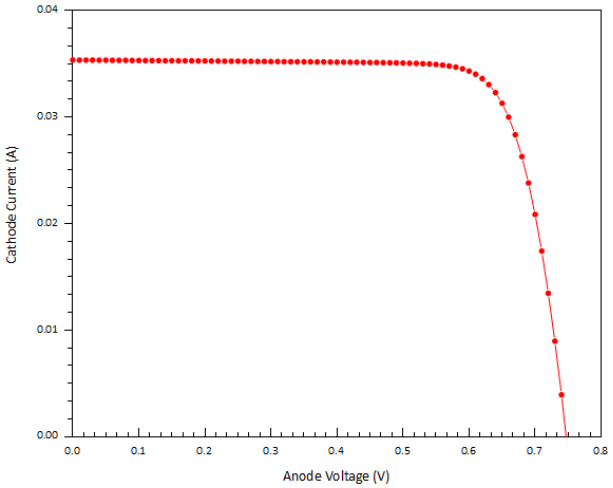

Figure 5. I-V characteristics curve of the TCAD model designed using Silvaco

IV. MODELLING OF ELECTRICAL CIRCUIT REPRESENTATION USING MATLAB

The electrical circuit to represent the TCAD model needs to have similar non-linear I-V characteristics curve to that of the TCAD model. Typically, the non-linear I-V characteristics curve of a solar cell as shown in Figure 6 is formed from three main points that are known as the short-circuit (0, I_{sc}), MPP (V_{mp}, I_{mp}), and open-circuit (V_{oc},0).

Recall from Figure 2 previously, there are three different circuit topologies available to represent solar cells. Compared to the one-diode model, the extra diode in the 2-diode model considers the recombination loss in the depletion region of the solar cell (Ishaque, Salam and Taheri, 2011). On the other hand, 3-diode model considers the influence of grain boundaries and large leakage current which requires more parameters to be calculated (Nishioka *et al.*, 2007). A higher number of diodes in the model indicates a more accurate representation but requires more complex computational effort. For the usage in this modelling approach, we chose the one-diode model because the model offers a good compromise between simplicity and accuracy (Villalva, Gazoli and Ruppert, 2009a). The validity of the one-diode model to represent solar cell is proven since the model had been used by previous researchers, some with more simplified version but the basic structure is always similar with a current source and a parallel diode (Bonkoungou *et al.*, 2013).

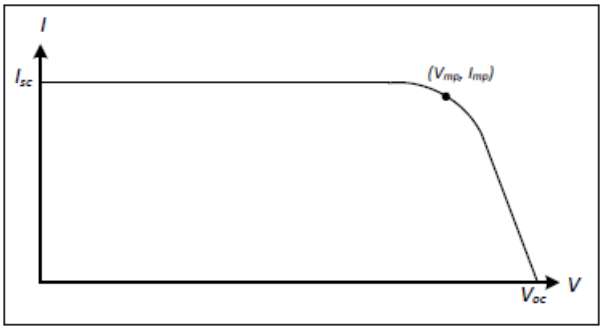

Figure 6. Non-linear I-V characteristics curve formed from the three main points

The I-V characteristics of the one-diode model is mathematically described as below (Rauschenbach, 1980).

$$I = I_{pv} - I_0 \left[e^{\left(\frac{V+R_s I}{V_t a}\right)} - 1 \right] - \frac{V+R_s I}{R_p} \quad (1)$$

where:

I_{pv} = PV current

I_0 = Diode reverse saturation current

V_t = Thermal voltage

α = Diode ideality constant

R_s = Equivalent series resistance

R_p = Equivalent parallel resistance

In equation (1), the thermal voltage, $V_t = {}^{kT}/_{q}$ where k is the Boltzmann constant which equals to $1.3806503 \times 10^{-23}$ J/K. This is followed by the temperature, T (measured in Kelvin) and the electron charge, q which equals to $1.60217646 \times 10^{-19}$ C. The equivalent series resistance, R_s and the equivalent parallel resistance, R_p is the total structural resistance of the device and resistance caused by the fabrication method of the solar cell respectively. These two resistances are a part of the internal characteristics of the solar cell. To calculate I_{pv} in equation (1), information on the parameters of the solar cell at nominal condition is

required. This includes the intensity of the solar irradiation, short-circuit current temperature coefficient, and the temperature (Sera, Teodorescu and Rodriguez, 2007).

$$I_{pv} = (I_{pv,n} + K_I \Delta_T) \frac{G}{G_n} \quad (2)$$

where:

$I_{pv,n}$ = Nominal PV current

K_I = Short-circuit current temperature coefficient

Δ_T = Difference between the actual and nominal temperature

G = Irradiation

G_n = Nominal irradiance

The diode reverse saturation current, I_0 requires the information on the short-circuit current and the open-circuit voltage as well as the open-circuit voltage temperature coefficient as elaborated below (Sera, Teodorescu and Rodriguez, 2007).

$$I_o = \frac{I_{sc,n} + K_I \Delta_T}{e^{([V_{oc,n} + K_V \Delta_T]/\alpha V_t) - 1}} \quad (3)$$

where:

$I_{sc,n}$ = Nominal short-circuit current

$V_{oc,n}$ = Nominal open-circuit voltage

K_V = Open-circuit voltage temperature coefficient

K_I = Short-circuit current temperature coefficient

Δ_T = Difference between the actual and nominal temperature

α = Diode ideality constant

The value of the diode constant, α may be chosen arbitrarily in the range of $1 \leq \alpha \leq 1.5$ depending on the other parameters of the non-linear I-V curve (Villalva, Gazoli and Filho, 2009). The value of α expresses how ideal the diode is and it affects the non-linear I-V curve of the one-diode model. Moreover, this constant can be modified to improve the accuracy of the model (Villalva, Gazoli and Filho, 2009).

The one-diode model is developed based on equations (1) – (3). Parameters such as $I_{sc,n}$, $V_{oc,n}$, I_{mp}, and V_{mp} are obtained from the TCAD model whereby the short-circuit current and open-circuit voltage temperature coefficients, K_I and K_V respectively are implemented based on the mean value obtained from datasheets of thin-film CIGS solar panel that are available commercially. Newton-Raphson iteration method is implemented to obtain the two unknown parameters which were the equivalent series and parallel resistances, R_s and R_p (Villalva, Gazoli and Filho, 2009). As a result, the non-linear I-V curves for the one-diode model and the TCAD model at nominal condition is shown in Figure 7. The I-V curves are plotted together to show how accurate was the one-diode model in representing the TCAD model.

In Figure 7, it can be observed that the one-diode model is able to reproduce the I-V curve of the TCAD model with great accuracy. They are exactly matched at the short-circuit (0, I_{sc}), MPP (V_{mp}, I_{mp}), and open-circuit (V_{oc},0). (0, Isc) points. This is because these points are the base points used to develop the one-diode model as described in equation (3). Aside from these three points, minimal error gaps are observed along the I-V curves. The error gaps might be improved slightly by using different values of α (Villalva, Gazoli and Ruppert, 2009b). However, optimization of α is not addressed in this work. Since the accuracy is up to 98%, we can conclude that the one-diode model is sufficient as a representation of the TCAD model.

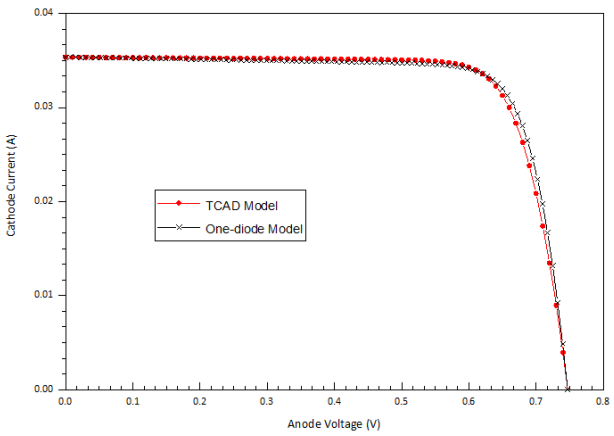

Figure 7. Non-linear I-V curve of one-diode model plotted against I-V curve of TCAD model at nominal condition

V. ONE-DIODE MODEL VALIDATION AT DIFFERENT TEMPERATURE

Further validation of the I-V curves was done across a wide range of temperature to observe the performance variation of the one-diode model. This is important since temperature variation might cause the accuracy of the one-diode model to drop. The chosen temperatures are 15°C, 25°C, and 75°C, which represents the lowest temperature in this region, temperature at STC, and the maximum temperature set by the Sustainable Energy Development Authority (SEDA) Malaysia respectively (SEDA Malaysia Grid-Connected Photovoltaic Systems Design Course, no date). Figure 8 depicts the I-V curves of the one-diode model plotted against the I-V curves of the TCAD model at three different temperatures.

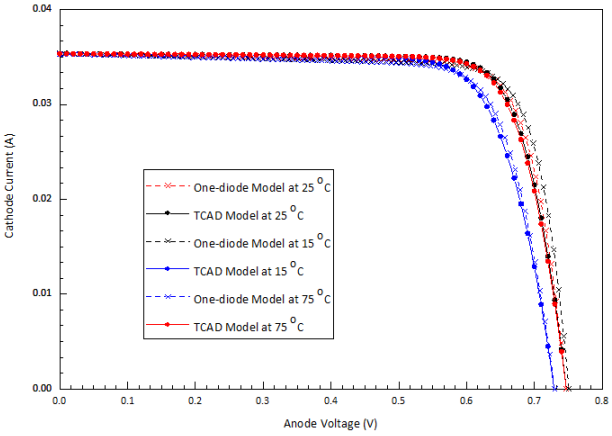

Figure 8. Non-linear I-V curves of one-diode model plotted against I-V curve of TCAD model across different temperatures

In Figure 8, the solid lines correspond to the I-V curves of the one-diode model of which the black color represents 15°C, red represents 25°C, and blue represents 75°C. On the contrary, the dashed line represents the I-V curves of the TCAD model with similar color coding for the different temperatures. From the figure, it can be observed that at each temperature, the curves are sufficiently accurate with exact match at the three main points denoted by the circular markers. In terms of accuracy, it was found that at 15°C and 25°C, the I-V curves were similarly accurate. However, at 75°C, the I-V curve of the one-diode model tends to deviate from the I-V curve of the TCAD model. The increase in deviation at high temperature is caused by the values of the temperature coefficients, K_I and K_V. If these values were obtained from the characterization process of the TCAD model, the deviation at higher or lower temperatures will be reduced. Again, with this observation, it is concluded that the one-diode model is sufficiently capable of representing the TCAD model for circuit-level simulations.

VI. CIRCUIT SIMULATION USING THE ONE-DIODE MODEL

The one-diode model can be implemented in circuit-level simulations but first, it needs to be upscaled accordingly to represent the I-V curve of a PV module. As described previously in Section 1, PV module is formed by a group of solar cells interconnected together. Typically, a solar panel is a combination of solar cells in series (N_s) and parallel (N_p) as shown in Figure 9. In order to upscale the one-diode model of the CIGS thin-film solar cell to represent a solar panel, several assumptions are made based on a commercially available thin-film CIGS solar panel.

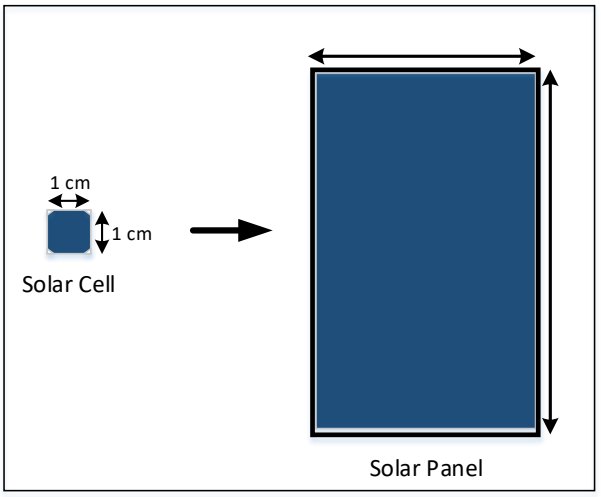

Figure 9. Solar cell versus solar module

A reference CIGS thin-film solar panel was chosen which is rated at 180W and the dimension of the solar panel is 1257 mm x 977 mm (*Solar Frontier K.K*). Currently, the record efficiency for a thin-film solar cell achieved by Solar Frontier is 22.9 % (John Parnell, 2017). Based on the latest solar panel datasheet there is an efficiency loss of approximately 40% when the solar cell from Solar Frontier is upscaled to the panel size. With this information, it is assumed that the one-diode solar cell efficiency will also drop by approximately 40% when upscaled to the size of a solar panel. Typically, the maximum output power of a solar panel is

$$P_{max} = V_{mp} \times I_{mp} \quad (4)$$

where:

V_{mp} = Voltage at MPP

I_{mp} = Current at MPP

Taking into account the efficiency loss, the adjusted maximum output power is

$$P_{adj} = V_{mp} \times I_{mp} \times Eff_{loss} \quad (5)$$

where:

Eff_{loss} = Efficiency loss

From equations (4), (5), and with the assumption that the one-diode model is relatively similar to the solar cell from Solar Frontier, the I-V curve and the P-V curve of the upscaled one-diode model can be obtained such as shown in Figure 10.

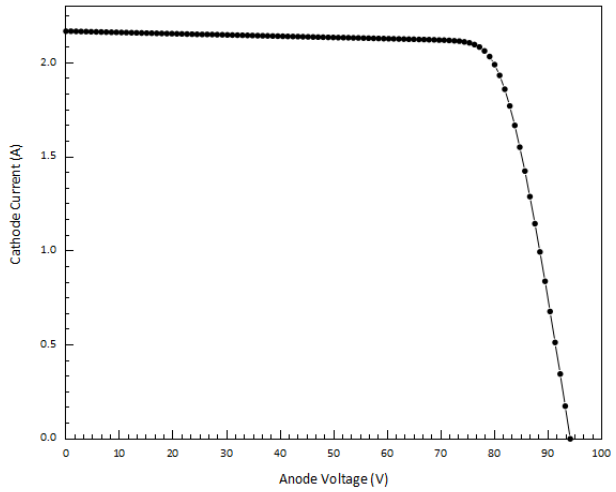

Figure 10. I-V curve of the upscaled one-diode model

In Figure 10, it is observed that the I_{sc}, V_{oc}, I_{mp}, and V_{mp} is 2.169 A, 94.12 V, 2.064 A, and 78.11 V respectively. The maximum output power of the upscaled one-diode model is 161.2 W which is comparable to the maximum output power of similar-sized solar modules. From here, the upscaled one-diode model can be implemented in system-level simulations in which the solar module performance is based on the designed TCAD model. Hence, this approach is applicable in research such as on the Maximum Power Point Tracking (MPPT) algorithms where the usual practice uses commercially available solar module data (Mohanty, Subudhi and Ray, 2016; Ahmed and Salam, 2018; Yilmaz, Kircay and Borekci, 2018). However, if any changes are to be made on the TCAD model, the one-diode model needs to be redeveloped as presented in this paper. For example, changing the doping concentration will affect the open-circuit voltage of the solar cell. Therefore, V_{oc} of the TCAD model will change and subsequently the equivalent one-diode model will change as well.

VII. CONCLUSION

In order to extend the simulation capability of a solar cell from cell level to the system level, a modelling approach is presented. It is an improvement over conventional modelling approach where the solar cell is represented by a one-diode model electrical circuit for the system level simulations. With this implementation, the impact on the system performance caused by changes in the solar cell materials can be observed.

Silvaco TCAD software is used to develop a thin-film CIGS solar cell model. Optimized baseline parameters such as layer thickness and doping concentration with respect to cells' efficiency are identified. They are selected based on prior researchers' simulations and experimental studies. The logfile from Silvaco TCAD contains the electrical properties of the TCAD model. An equivalent one-diode electrical model is developed in order to act as the TCAD model for circuit-level simulations.

The performance of the one-diode model to represent the TCAD model is validated at different temperatures. It is observed that the non-linear I-V curve of the one-diode model is able to represent the non-linear I-V curve of the TCAD model with great accuracy across the temperature range. Minimal error gaps are still observable along the I-V curve, and it is expected due to the limitation of the one-diode model. Higher accuracy can be achieved by implementing more detailed models such as the 2-diode model and 3-diode model, but with a higher level of complexity in return. In order to implement the one-diode model at circuit-level simulation, upscaling is required since the one-diode model represents a solar cell instead of a solar panel. Some assumptions are made relatively to the current thin-film solar panel in order to upscale the one-diode model to achieve the performance of a solar panel.

VIII. REFERENCES

Abdul, M *et al.* 2012, 'Modeling, simulation and optimization of high performance CIGS solar cell', *International Journal of Computer Applications*, vol. 57, no.16, pp. 26-30.

Ahmed, J & Salam, Z 2018, 'An enhanced adaptive p&o mppt for fast and efficient tracking under varying environmental conditions', *IEEE Transactions on Sustainable Energy*, vol. 9, no. 3, pp. 1487-1496.

Benmir, A & Aida, M S 2013, 'Analytical modeling and simulation of CIGS solar cells', *Energy Procedia*, vol. 36, pp. 618–627.

Bonkoungou, D *et al.* 2013, 'Modelling and simulation of photvolotaic module considering single-diode equivalent circuit model in MATLAB', *International Journal of Emerging Technology and Advanced Engineering*, vol. 3, no.3, pp. 493-502.

Dabbabi, S, Nasr, T Ben & Kamoun-Turki, N 2017, 'Parameters optimization of CIGS solar cell using 2D physical modeling', *Results in Physics*, vol. 7, pp. 4020–4024.

Fathil, M F M *et al.* 2014, 'The impact of minority carrier lifetime and carrier concentration on the efficiency of cigs solar cell', *IEEE International Conference on Semiconductor Electronics (ICSE2014)*, pp. 24-27.

Green, M A *et al.* 2018, 'Solar cell efficiency tables (version 51)', *Progress in Photovoltaics: Research and Applications*, vol. 26, no. 1, pp. 3–12.

Heriche, H, Rouabah, Z & Bouarissa, N 2016, 'High-efficiency CIGS solar cells with optimization of layers thickness and doping', *Optik*. vol. 127, no. 24, pp. 11751–11757.

Ishaque, K, Salam, Z & Taheri, H 2011, 'Simple, fast and accurate two-diode model for photovoltaic modules', *Solar Energy Materials and Solar Cells*, vol. 95, no. 2, pp. 586–594.

John Parnell 2017, *Solar Frontier breaks thin-film efficiency record with lab-scale cell*, *PV Tech*., viewed 31 January 2019, <https://www.pv-tech.org/news/solar-frontier-breaks-thin-film-efficiency-record-with-lab-scale-cell>.

Khoshsirat, N *et al.* 2015, 'Analysis of absorber layer properties effect on CIGS solar cell performance using SCAPS', *Optik*, vol. 126, no. 7–8, pp. 681–686.

Mohanty, S, Subudhi, B & Ray, P K 2016, 'A new MPPT design using grey Wolf optimization technique for photovoltaic system under partial shading conditions', *IEEE Transactions on Sustainable Energy*, vol. 7, no. 1, pp. 181-188.

Mostefaoui, M *et al.* 2015, 'Simulation of high efficiency cigs solar cells with SCAPS-1D software', *Energy Procedia*. vol. 74, pp. 736–744.

Nishioka, K *et al.* 2007, 'Analysis of multicrystalline silicon solar cells by modified 3-diode equivalent circuit model taking leakage current through periphery into consideration', *Solar Energy Materials and Solar Cells*. vol. 91, no. 13, pp. 1222–1227.

Rauschenbach, H S 1980, *Solar Cell Array Design Handbook*, Springer Netherlands.

Sera, D, Teodorescu, R & Rodriguez, P 2007, 'PV panel model based on datasheet values', *IEEE International Symposium on Industrial Electronics*, pp. 2392–2396.

Shamim, S M *et al.* 2015, *Performance analysis on the effect of doping concentration in copper indium gallium selenide (CIGS) thin-film solar cell*, *International Journal of Computer Applications*, vol. 113, no. 14.

Solar Frontier K K, viewed 29 January 2019, <www.solar-frontier.com>.

Sylla, A, Touré, S & Vilcot, J P 2017, 'Numerical modeling and simulation of cigs-based solar cells with ZnS buffer layer', *Open Journal of Modelling and Simulation*. vol. 5, no. 4, pp. 218–231.

Villalva, M G, Gazoli, J R & Ruppert, E F 2009, 'Modeling and circuit-based simulation of

photovoltaic arrays', *Brazilian Power Electronics Conference,* pp. 1244–1254.

Villalva, M G, Gazoli, J R & Ruppert, E F 2009, 'Comprehensive approach to modeling and simulation of photovoltaic arrays', *IEEE Transactions on Power Electronics*, vol. 24, no. 5, pp. 1198–1208.

Yilmaz, U, Kircay, A & Borekci, S 2018, 'PV system fuzzy logic MPPT method and PI control as a charge controller', *Renewable and Sustainable Energy Reviews*. vol.81, pp. 994–1001.

Za'abar, F *et al.* 2018, 'Optimization of baseline parameters and numerical simulation for Cu(In, Ga)Se2 solar cell', *IEEE International Conference on Semiconductor Electronics (ICSE2018)*, pp. 209–213.